

HYDRODYNAMIC SIMULATIONS OF CHENIER PLAIN LAKES

Saikiran Yadagiri, Yang Zhou, Ning Zhang*

Department of Engineering
McNeese State University
Lake Charles, LA 70609, USA

* Corresponding Author: nzhang@mcneese.edu

Abstract

This paper is about the hydrodynamic simulations on Chenier Plains. The Chenier plain is a rich and complex mixture of wetlands, uplands and open water that extends from Vermilion Bay, Louisiana, to Galveston Bay, Texas. Chenier Plains is a Source water supply to the surrounding wetlands and critical to the health of wetlands. Chenier Plains consists of white, Grand, Calcasieu and Sabine lakes. In this Paper we mainly concentrate on Calcasieu and Sabine Lake. To study about this lake, numerical simulations were conducted. A depth Averaged shallow water equation is used to simulate the hydrodynamics. Using these simulations we have computed the velocity, water level and the associated flooding due to the change of water level around the lake for duration of one month. The results have been compared with the measurement data (southwest Louisiana national wildlife refuge complex and National Oceanic and Atmospheric Administration). The results agreed well with the measurement data.

Introduction

The simulation of 2-d shallow water equations is involved by lot of environment and engineering problems. One of the main difficulty in the simulation and analysis is the unsteady flow of the lakes and oceans. In this paper the simulation and the analysis of the lakes is described by the Semi-Implicit Finite Difference Methods for the Two-Dimensional Shallow Water Equations¹.

The system of the shallow water equations is the hyperbolic problem at the core of many problems for the dynamics of the ocean or atmosphere. The shallow water equations can be numerically solved by finite difference^{1,2,3}, finite element^{4,5} and finite volume methods^{6,7}. Besides the finite element method the staggered grid method and cell centered-finite volume is largely applied around the world. The staggered grid method is descritized by the implicit method^{1,8} and the cell centered –finite volume is descritized by the explicit time method⁹. The implicit approximation of the integral leads to the better stability properties of the scheme in comparison with the explicit time integration. In fact, explicit schemes for the shallow water equations must follow CFL condition¹⁰. The shallow water equations model the propagation of disturbances in water and other incompressible fluids. The underlying assumption is that the depth of the fluid is very small compared to the wave length of the disturbance. Typical physical situations modeled by the shallow water equations are therefore tidal waves, the currents in

portual basins, the atmospheric circulation. The area of interest of our study in this paper is on the Chenier plain lakes. In this paper we focus on unsteady simulation of Sabine Lake and steady state simulation Calcasieu Lake.

Numerical Method

The physical domain is discretized into grid cells for numerical resolution. This method can be used for rectangular shape grids. Structured Cartesian grids are simple and very effective. Here a implicit finite difference staggered grid is used for the formulation. Explicit method is used to calculate the state of a system at a later time from the state of the system at the current time, while implicit methods find a solution by solving an equation involving both the current state of the system and the later one. It is clear that implicit methods require an extra computation and they are much harder to implement. Implicit methods are used because many problems arising in practical conditions are stiff, for which the use of an explicit method requires impractically small time steps to keep the error in result bounded. In this situation to get better accuracy it will take less computational time to use an implicit method with larger time steps.

Governing Equations

The equations are derived from the principles of conservation of mass and conservation of momentum under the shallow water hypothesis. This implies a depth averaged process in the equations and is associated to the assumption of hydrostatic pressure vertical distribution. The 2-d shallow water equations¹¹ are below Eq. (1),(2),(3).

$$\frac{\partial h}{\partial t} + \frac{\partial(uh)}{\partial x} + \frac{\partial(vh)}{\partial y} = 0 \quad \text{Eq.(1)}$$

$$\frac{\partial(uh)}{\partial t} + \frac{\partial(u^2h + \frac{1}{2}gh^2)}{\partial x} + \frac{\partial(uvh)}{\partial y} = 0 \quad \text{Eq.(2)}$$

$$\frac{\partial(vh)}{\partial t} + \frac{\partial(uvh)}{\partial x} + \frac{\partial(v^2h + \frac{1}{2}gh^2)}{\partial y} = 0 \quad \text{Eq.(3)}$$

In the above equations u and v are the velocities along x and y direction. H is the total depth. h is the elevation over horizontal reference plane and h_0 is the depth the reference plane. C is the chezy coefficient, g is the acceleration of gravity, l is the corolis parameter. P_a is the atmospheric pressure at the free surface, ρ is the density which assumed as constant, μ is the diffusion coefficient

Results and Comparisons

Steady state simulation of Calcasieu lake

Theory and background:

The two-dimensional shallow water equations are the governing equations in this study^{12,13}. The variables to be solved are the two velocity components and water-surface elevation. The area of interest includes the whole Calcasieu Lake, Calcasieu River which is at the north of the lake and small portion of Gulf of Mexico which is outlet of the lake called Calcasieu Pass. The total area is 1156 km². Chezy friction coefficient is calculated as 71.3 while the average depth of the lake is about 1.5m. The time step used in the simulation is fixed at 1 min, which is much smaller than the required stability condition.

Grid-Independence Check:

The computational domain is a rectangular domain which has size about 45km x 26km. A 174x100 grid mesh is placed on the domain. The number of mesh points is determined by comparing the results of 174x100 to the results of a finer mesh 348x200. There is no difference between two results indicates the 174x100 mesh is fine enough for the simulation.

Steady-State Simulation:

To check the convergence of the solutions, the steady-state simulation has been performed. The inlet flow rate is specified as 178m³/s¹⁴, while the outflow open boundary is specified at Gulf of Mexico water. For steady-state simulation, eventually, the outflow rate should be equal to the inlet flow rate. Figure (1) is the history of inlet and outlet flow rate, and it is clear that the outflow rate converged to 178m³/s. The satisfactory of the convergence indicates the accuracy of the steady-state simulation.

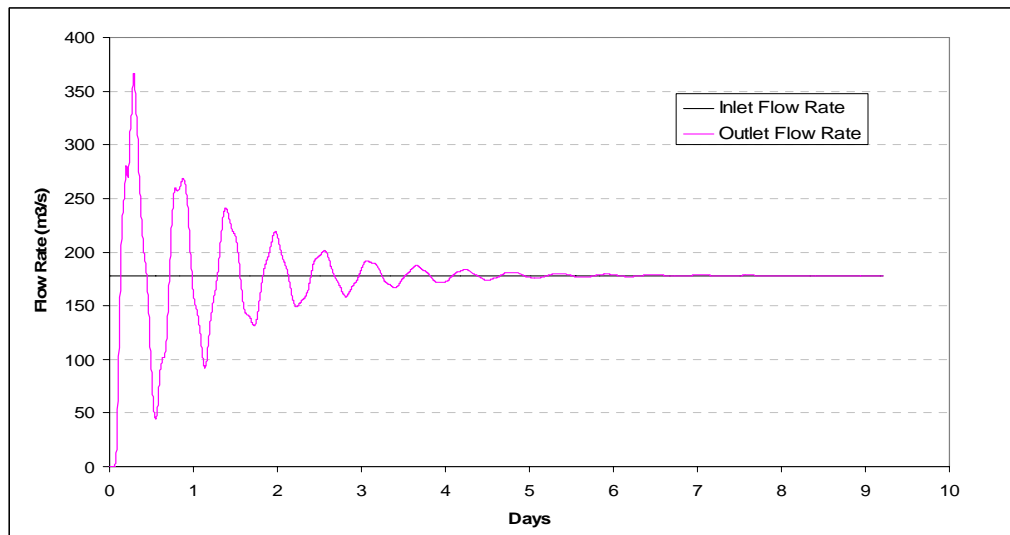


Figure 1, Flow Rate History for Steady-State Case

Unsteady state simulation of Sabine Lake Area

Simulation Setups

The average depth of the lake is about 1.0m. The computational domain is a rectangular area including the whole Sabine Lake and the surrounding wetlands, shown in Figure 2(a). The total area is about 1569 km². There are two major river inputs in the north of the lake, Sabine River and Neches River with a flow rate of 234.6m³/s and 278.7m³/s respectively. The lake outlet to the Gulf of Mexico is at the south of the lake, and called Sabine Pass. The topology data (elevation) of the lake bottom as well as the surrounding lands were obtained from NOAA Satellite and Information Service¹⁵. This is the difference comparing to the Calcasieu Lake case which only lake bottom elevation is available. From Figure 2, we can clearly observe the elevation of the lands surrounding the Sabine Lake. The high land at the north west corner of the domain is the city of Port Arthur, where the other relative flat lands are the wetlands. The wetlands at the left of the lake are in the McFaddin National Wildlife Refuge and J.D. Murphree Wildlife Management Area, while the wetlands in the right belong to the Sabine National Wild Life Refuge, and further right is the Calcasieu Lake. With the land data, we can simulation the flooding of the wetlands near the Sabine Lake. The computation domain is covered with a 200x150 mesh. Again, the depth data of the Sabine Ship Channel were absent from the database. Therefore, the ship channel was manually interpolated onto the grid mesh, shown in Figure 2(b). The averaged depth of the ship channel is about 12m¹⁶. All the simulations performed in this study include the ship channel, which is the current condition. Since we have land elevation data, we can see the flooding of the wetlands in this case, which is one of the major purposes in this case. Since steady state simulations were validated using Calcasieu Lake case, only unsteady simulations using actual ocean input data from May 1st to May 31st 2009 were conducted, and focus is on the water-surface elevation and flooding of wetlands.

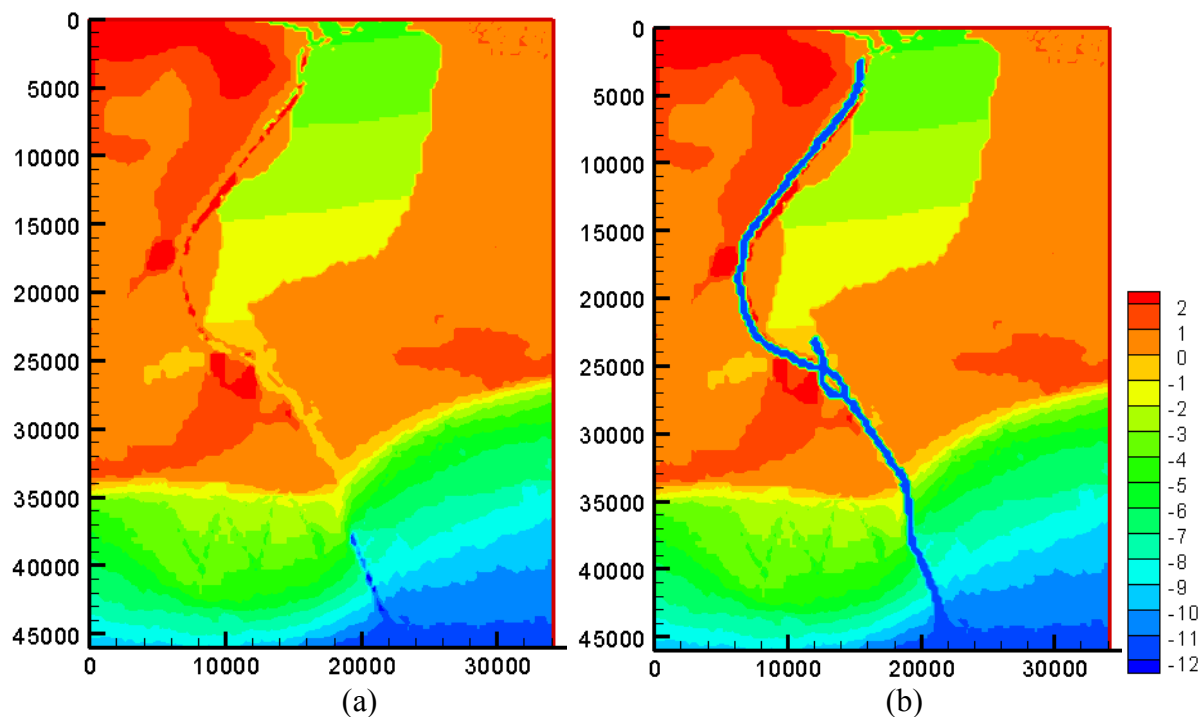


Figure 2, Geometry of Sabine Lake, Mapped on the Computational Grid

Unsteady Simulation:

Since the ocean surface level changes with time, the simulation becomes fully unsteady. A set of water-surface level data measured at the exit of the Sabine Pass from NOAA¹⁷ was used as ocean surface elevation boundary condition of the simulation. The water-surface elevation in the lake, at a location near Port Arthur, was actually measured by NOAA Port Arthur Station¹⁷ for the same period of time. The simulated water surface elevation of the same location were monitored and recorded during the simulation. The simulation results were compared with measurement data at that location along with the ocean data, shown in Figure 3. Figure 3 is the first 15 days of May 2009 water-surface elevation comparison with the measurement. Although the simulation results over-predict the water-surface elevation, the overall agreement is reasonably good. The periods of both simulation and measurement data show a little delay comparing with the ocean tidal periods, which is due to the time the tidal waves travel from ocean to the lake. More importantly, in the lake, the oscillating magnitude is a little smaller than the ocean tidal magnitude, but not much. The lake water level is very sensitive to the change of ocean water level, which means the area offers little protection to the nearby cities from the ocean. Again, the wide and deep ship channel, which causes great water exchanges between the lake and the ocean, is the major reason. Much smaller oscillation of the surface level can be observed without the ship channel.

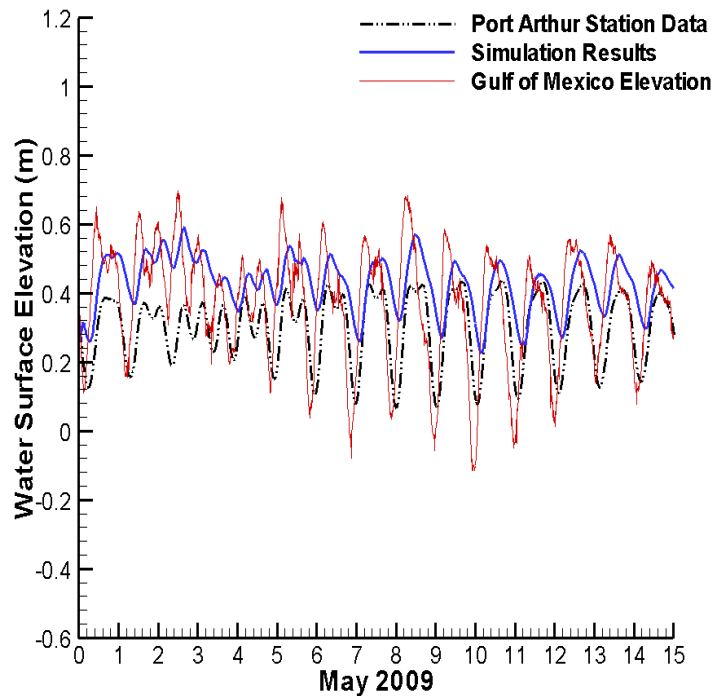
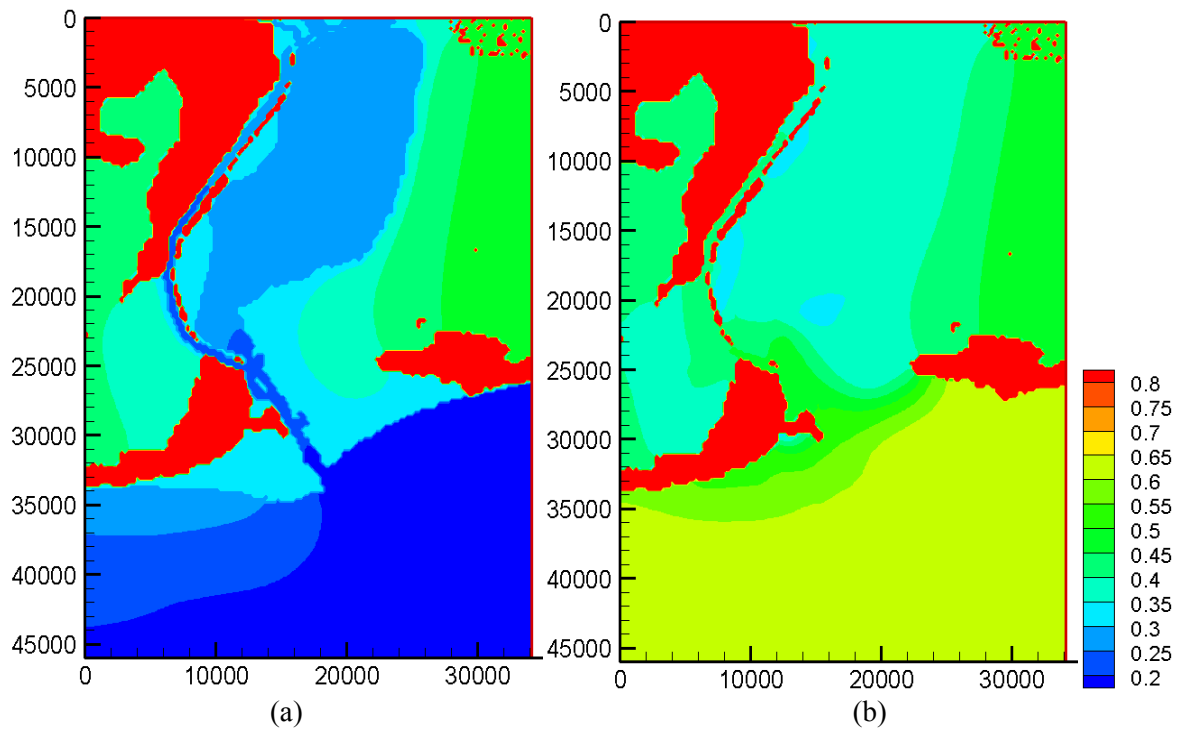


Figure 3, Water-Surface Elevation History Comparing to the Measurement

Another interesting aspect of Sabine Lake case is to see the flooding of wetlands at high tide. Because we have the land elevation data for this case, if the lake water level is higher than the land elevation which is about 1ft, flooding of wetlands occurs. Figure 4 shows the water surface elevation contours at high tide and low tide. At the ocean low tide Figure 4(a), the lake water level is low and the wetlands are not flooded. At the ocean high tide Figure 4(b), ocean water

starts to flow into the lake, the lake surface elevation increases, but not the highest since the time delay, and flooding to the wetlands starts. Then, ocean level starts to decrease Figure 4(c), however the lake surface level is the highest at this moment, and wetlands are flooded completely. Finally Figure 4(d), further decreasing of the ocean level causes further retreats of lake water, the lake starts to show its border again and wetlands starts to appear again. Figure 5(a) and 5(b) clearly says that the directions of vectors are towards when there is a high tide in the ocean and directions of the vectors are towards ocean when there is low tide in the ocean.



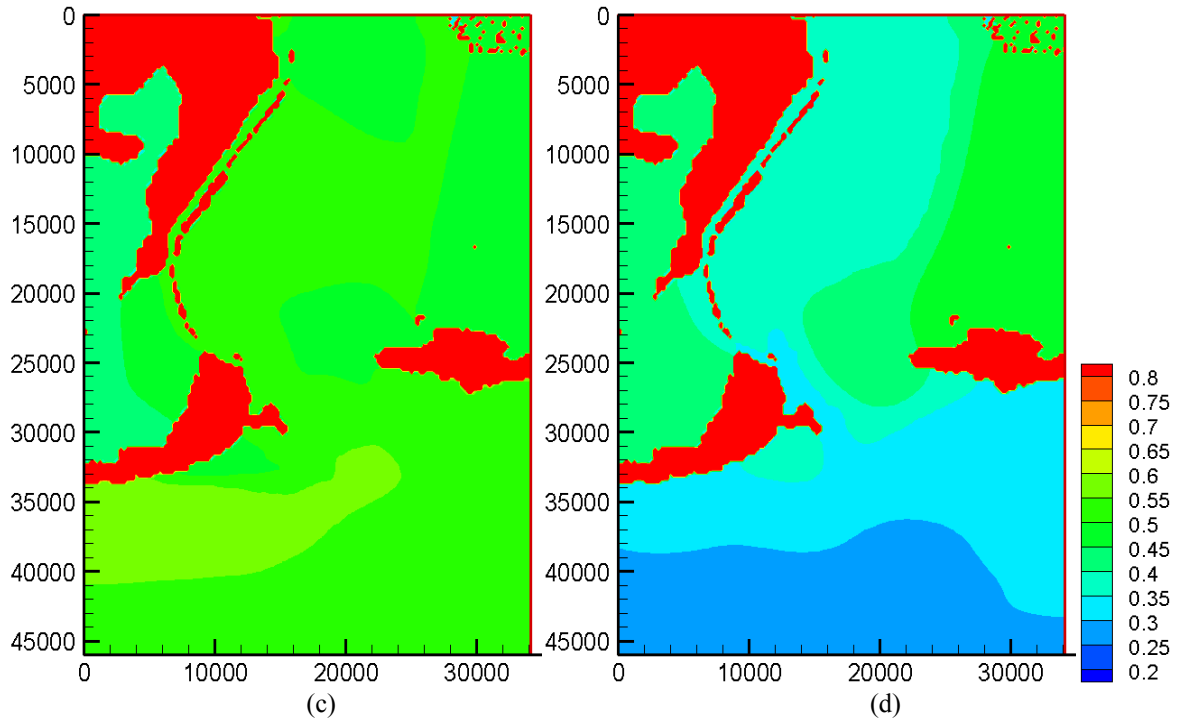


Figure 4, water-surface elevation contours showing the flooding of wetlands, (a) low tide in the ocean; (b) high tide in the ocean; (c) lake water retreats; (d) lake water further retreats

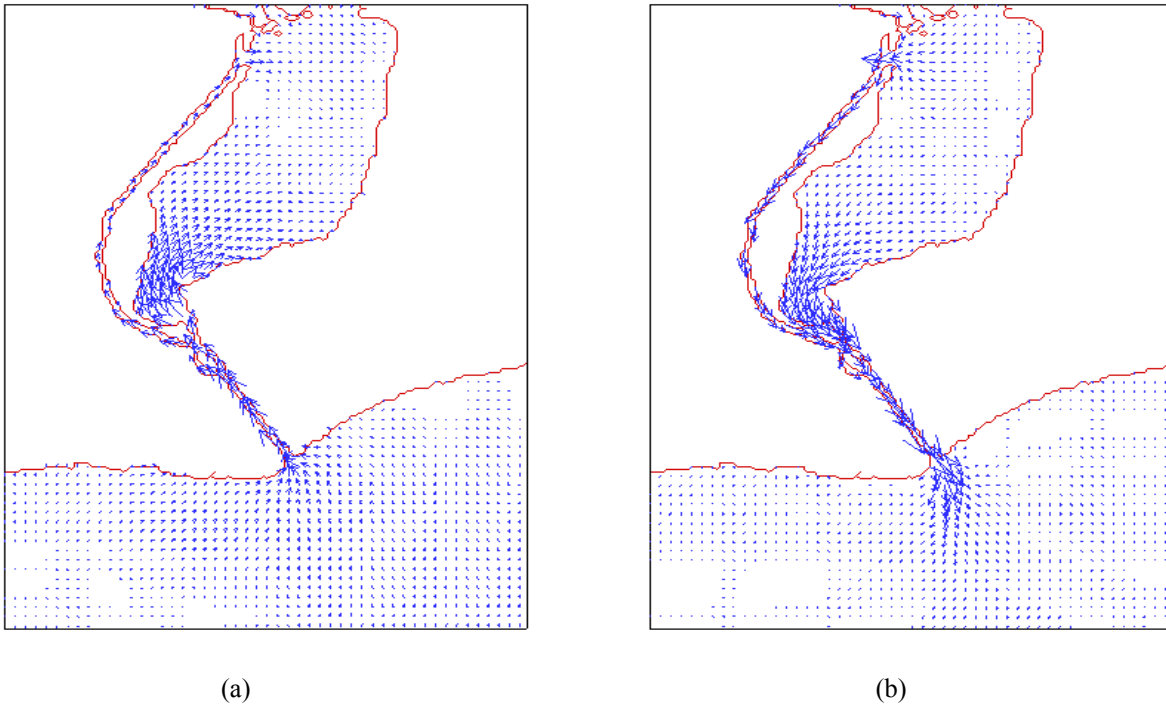


Figure 5, (a) vector field when high tide in the ocean; (b) vector field when low tide in the ocean

Summary and Conclusions

In this paper we have shown an application of our method for simulating shallow water equations. The region of simulation for Sabine Lake is 46km x 34.109km. The time step used in simulation is 1min. The numbers of grid points for Sabine lake is 200 x 150. Figure 2 is Sabine Lake mapped on computational grid. Figure 4 is water surface elevation contours of Sabine Lake. Figure 3 is the comparison of water surface elevation at Port Arthur with the actual measurement data for first 15 days of may 2009. In figure 3 we see that simulated results well agreed with actual measured data. When there is low tide in both lakes then water flows into the lake from the ocean and the water flowing through the rivers in to the lake is stopped. When there is high tide in both lakes then water flows from lake to the ocean and there is no ocean water flowing in to the lake. Because of both the ship channels in Calcasieu and Sabine lake water is flowing more freely in to the lake, brings more salt water into the lakes which effects on the salinity and nutrients of the surroundings wetlands. Vector field in figure 5 also shows that ship channel is effective and the majority of the water flowing to and from the lake is through the ship channel. In order to maintain the salinity and nutrients of the surrounding wetlands, some Dikes and channel barriers can be constructed to prevent the flooding in to the wetlands when there is high tide in the ocean.

References

1. V. Casulli, 1990, "Semi-Implicit Finite Difference Methods for the Two-Dimensional Shallow Water Equations", *Journal of Computational Physics*, Vol. 86, pp. 56-74
2. David A Randall, 1993 "Geostrophic adjustment and the finite-difference shallow water equations".
3. A.I.Delis and Th.Katasaounis, 1998 "numerical solution of the two-dimensional shallow water equations by the application relaxation methods"
4. A.Bermudez, C.Rodriguez and M.A.Vilar "solving shallow water equations by a mixed implicit finite element Method"
5. Shin-Jye Liang, Jyh-jaw tang and Ming-Shun Wu, 2006 " solution of shallow water equations using least – squares finite element method"
6. J.Fe,F.navarrina &J.puertas, " A finite volume model for the resolution of the shallow water equations with moving boundary conditions"
7. C.G.Mingham and D.M.Causon, 1998" high-resolution finite-volume method for shallow water flows"
8. R.L.Stockstill, 1996 "implicit moving finite element model of the 2d shallow water equations"
9. A.Valiani,V.Caleffi, A.Zanni,1998" finite volume scheme for 2d shallow water equations application to the malpassetdam-break"
10. E.Turkel, G.Zwas,1996 " explicit large time-step schemes the shallow water equations:
11. V.I.Agoshkov,A.Quarteroni,F.Saleri, 1994, 175-200 "recent developments in numerical simulation shallow water equations I .boundary equations"
12. R.E. Spall, C. Addley, and T. Hardy, 2001, "Numerical Analysis of Large, Gravel-Bed Rivers Using the Depth Averaged Equations of Motion", Proc. of 2001 ASME Fluids Engineering Division Summer Meeting, New Orleans, LA
13. Z.C. Zheng and N. Zhang, 2002, "A Hydrodynamic Simulation for Mobile Bay Circulation", Proc. of 2002 International Mechanical Engineering Congress & Exposition, New Orleans, LA
14. Resource Database for Gulf of Mexico Research, <http://www.GulfBase.org>
15. NOAA Satellite and Information Service, National Geophysical Data Center, <http://www.ngdc.noaa.gov/mgg/global/global.html>
16. Sabine Pass LNG, L.P., 2009, "Environmental Assessment, Sabine Pass LNG Export Project Report", US Department of Energy, DOE/EA-1649
17. Center for Operational Oceanographic Products and Services, National Oceanic and Atmospheric Administration (NOAA), <http://tidesandcurrent.noaa.gov>